

Supplementary Figures for

**Dissecting caspase-2-mediated cell death: from intrinsic
PIDosome activation to chemical modulation**

Mengxue Zeng, Kun Wang, Qingcui Wu, Jingjin Ding, Dan Xie, Xiangbing Qi,
and Feng Shao

This file contains: Figure S1 to S5

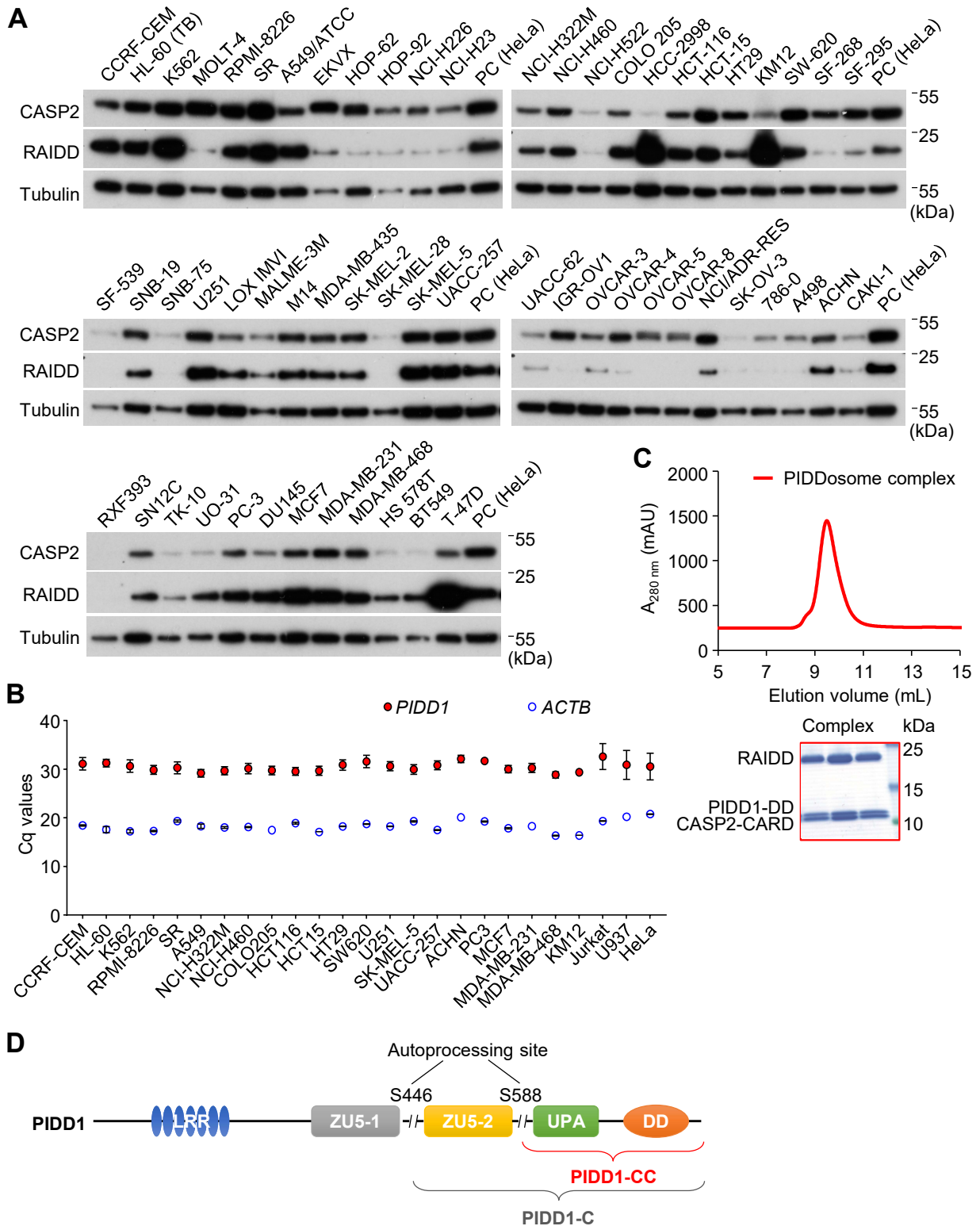


Figure S1. Profiling endogenous caspase-2 and RAIDD expression in the NCI-60 and biochemical characterization of the PIDDosome complex.

(A) Lysates of 60 cancer cell lines from the NCI-60 (a panel of 60 diverse human cancer cell lines used by the US National Cancer Institute to screen and evaluate anti-cancer drugs) were analyzed by immunoblotting using indicated antibodies. Wild-type HeLa cell lysate was included as a positive (PC). (B) *PIDD1* expression was profiled by quantitative real time reverse transcription polymerase chain reaction (qRT-PCR) in indicated cell lines. *ACTB* expression was measured in parallel as a constitutive reference with high expression. (C) Gel-filtration chromatography analysis of the PIDDosome complex formed by PIDD1 death domain (PIDD1-DD), full-length RAIDD and caspase-2 CARD domain (CASP2-CARD), along with SDS-PAGE analysis of the complex in the elution peak fractions. (D) Schematic diagram of PIDD1 domain organization. Data in (A–C) are representative of three independent experiments.

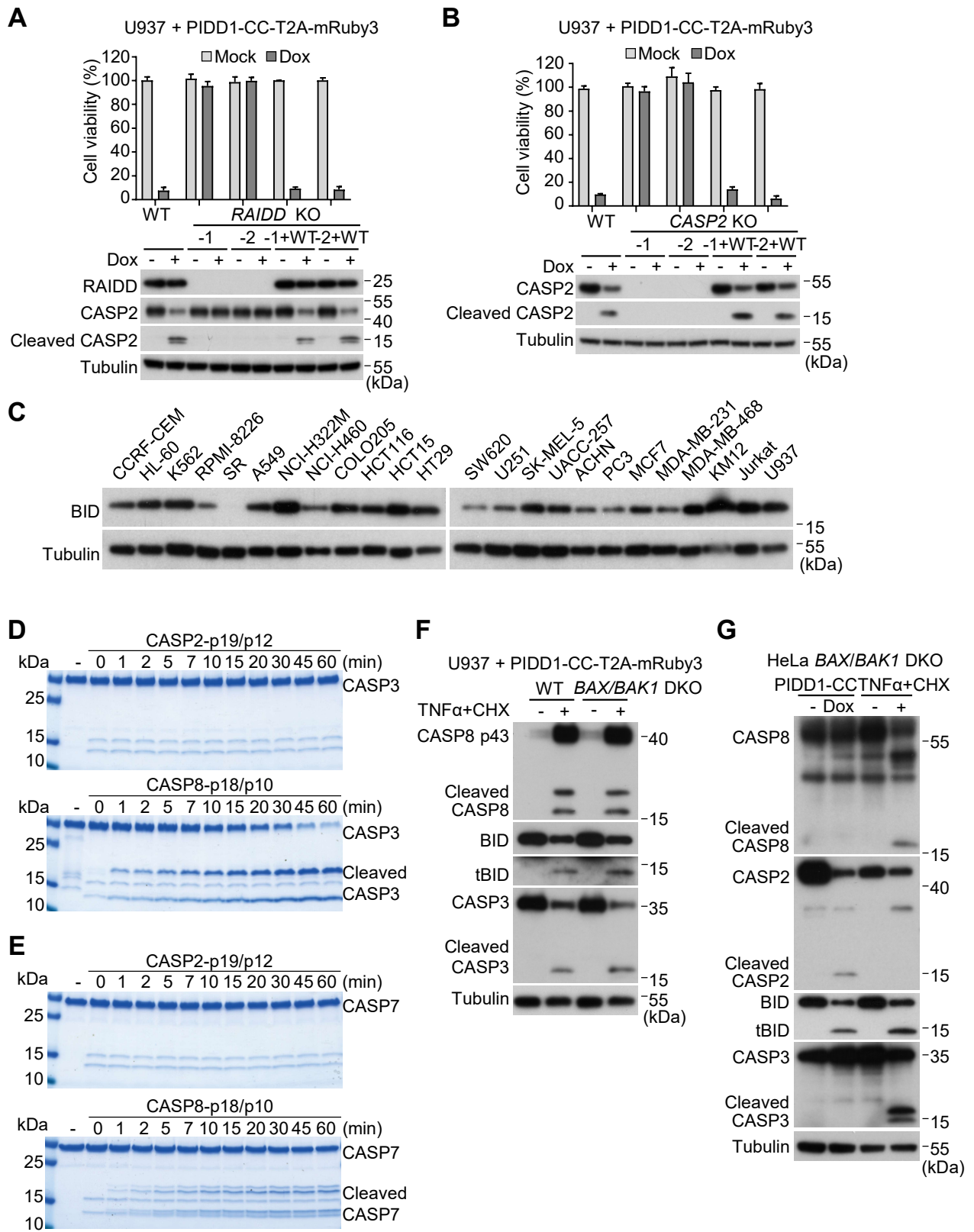


Figure S2

Figure S2. Profiling the differences between caspase-2 and caspase-8 in BID and caspase-3 processing.

(A and B) RAIDD and CASP2 are both essential for PIDD1-CC-induced caspase-2 activation and cell death in U937 cells. Two *RAIDD*^{-/-} (KO) clones (A) and two *CASP2*^{-/-} (KO) clones (B) of U937 cells, as well as the knockout clones complemented with wild-type (WT) RAIDD and caspase-2, respectively, were stimulated by dox-induced expression of PIDD1-CC for 11 h. ATP-based cell viability is expressed as mean \pm s.d. from three technical replicates. Immunoblotting detecting caspase-2 processing is shown. (C) Immunoblots of endogenous BID expression in the 22 RAIDD/CASP2 double-positive cancer cell lines assayed in Fig. 1A. (D and E) *In vitro* cleavage of caspase-3/7 by active form of caspase-8 but not caspase-2. Purified caspase-3-C163A (D) or caspase-7-C186A (E) proteins were incubated with active caspase-2 and caspase-8 proteins for indicated time, and the samples were subjected to SDS-PAGE analysis. (F) Validation of the roles of BAX and BAK in caspase-8-mediated BID and caspase-3 processing by immunoblotting. WT and *BAX*^{-/-}*BAK*^{-/-} (DKO) U937 cells were treated with TNF α plus cycloheximide (CHX) for 2 h to activate caspase-8. (G) Differential roles of BAX and BAK in caspase-2 and caspase-8 activation-mediated processing of BID and caspase-3. WT and *BAX*^{-/-}*BAK*^{-/-} (DKO) HeLa cells were stimulated by dox-induced expression of PIDD1-CC for caspase-2 activation or TNF α plus CHX treatment for caspase-8 activation. Processing of caspase-2, -3, and -8, and BID was analyzed by immunoblotting. All data are representative of three independent experiments.

Gene	gRNA	FC_recover	Ranking
<i>BID</i>	BID_4	771.5143	1
<i>BID</i>	BID_1	765.6589	2
<i>BID</i>	BID_6	748.5108	3
<i>BID</i>	BID_5	747.0161	4
<i>BID</i>	BID_3	507.1263	6
<i>BID</i>	BID_2	359.9454	11
<i>CASP2</i>	CASP2_2	523.174	5
<i>CASP2</i>	CASP2_3	499.6242	7
<i>CASP2</i>	CASP2_1	387.4627	10
<i>CASP2</i>	CASP2_6	239.9944	13
<i>CASP2</i>	CASP2_5	152.3754	15
<i>CRADD</i>	CRADD_6	423.511	8
<i>CRADD</i>	CRADD_2	404.5781	9
<i>CRADD</i>	CRADD_1	257.0858	12
<i>CRADD</i>	CRADD_3	235.3633	14
<i>CRADD</i>	CRADD_4	25.89795	19
<i>DDIT4</i>	DDIT4_6	25.65607	88
<i>DDIT4</i>	DDIT4_2	10.56757	430
<i>DDIT4</i>	DDIT4_4	8.342154	710
<i>DDIT4</i>	DDIT4_5	7.615992	845
<i>DDIT4</i>	DDIT4_1	5.279328	1615
<i>DET1</i>	DET1_6	9.074155	596
<i>DET1</i>	DET1_5	7.724657	817
<i>DET1</i>	DET1_4	7.398984	897
<i>DET1</i>	DET1_2	5.594437	1462
<i>FLCN</i>	FLCN_2	13.99241	247
<i>FLCN</i>	FLCN_3	10.46674	443
<i>FLCN</i>	FLCN_6	8.373865	701
<i>FLCN</i>	FLCN_5	7.964379	764
<i>LAMTOR2</i>	LAMTOR2_5	9.797291	504
<i>LAMTOR2</i>	LAMTOR2_6	7.710842	820
<i>LAMTOR2</i>	LAMTOR2_3	7.058851	986
<i>LAMTOR2</i>	LAMTOR2_2	6.09096	1273
<i>PTBP1</i>	PTBP1_3	106.188	24
<i>PTBP1</i>	PTBP1_2	25.52036	89
<i>PTBP1</i>	PTBP1_5	13.61567	264
<i>PTBP1</i>	PTBP1_4	8.184038	725
<i>PTBP1</i>	PTBP1_1	7.963278	765
<i>RRAGA</i>	RRAGA_3	10.39173	450
<i>RRAGA</i>	RRAGA_2	6.674335	1093
<i>RRAGA</i>	RRAGA_6	5.32618	1593
<i>RRAGA</i>	RRAGA_1	5.255568	1629
<i>RRAGA</i>	RRAGA_5	4.972998	1795

Figure S3. CRISPR-Cas9 screen of PIDD1-CC-induced cell death.

U937 cells harboring PIDD1-CC-T2A-mRuby3 and ZsGreen were treated with doxycycline to induce PIDDosome-stimulated apoptosis. The pool of RFP/GFP-double-positive cells were subjected to gRNA sequencing to identify enriched clones. Among the top 2,000 gRNA hits, 9 genes were hit by four or more gRNAs, but only RAIDD, CASP2, and BID passed subsequent validation using their knockout cell lines.

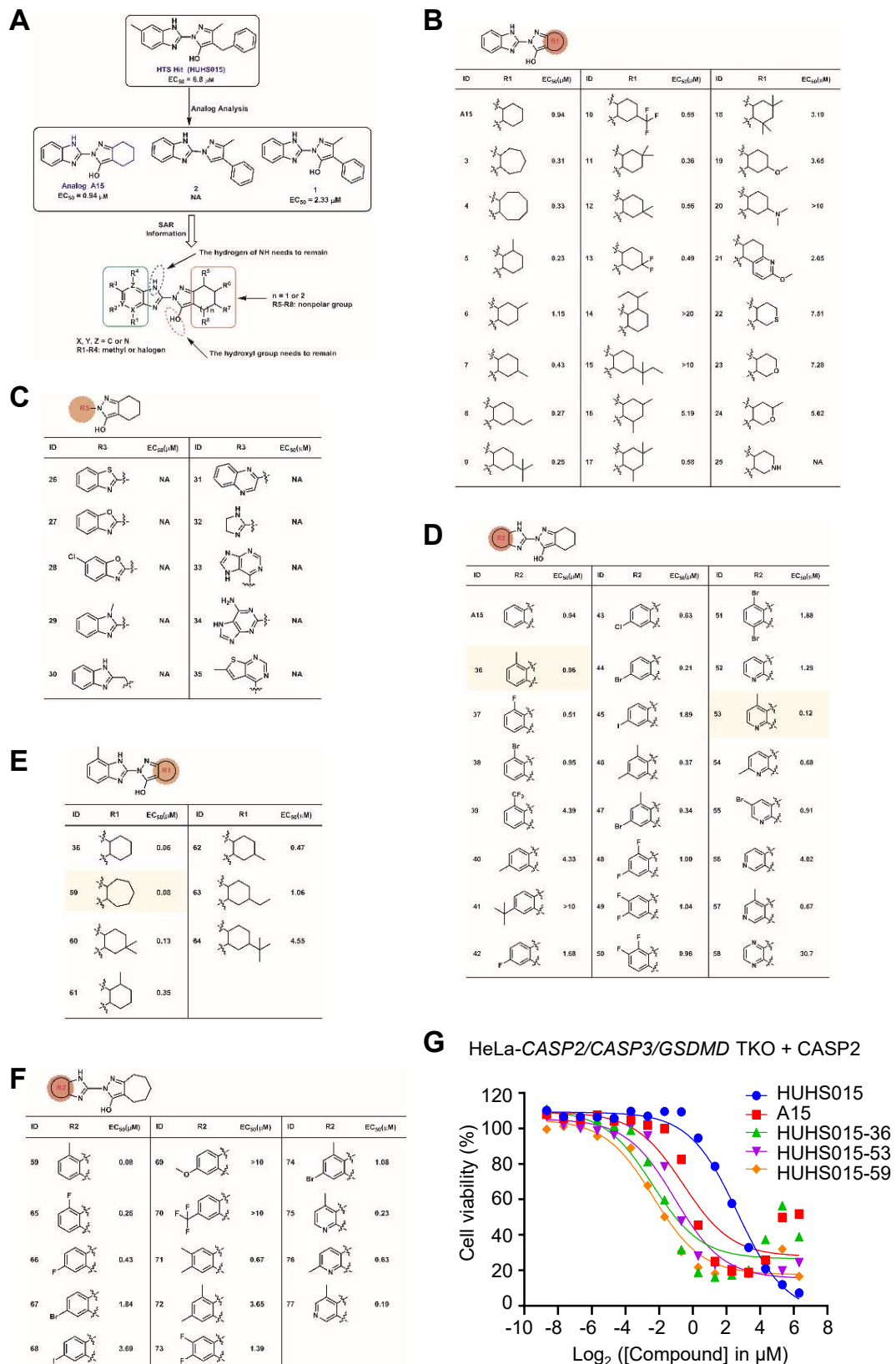


Figure S4

Figure S4. Structure-Activity Relationship analyses of HUHS015 and its derivatives.

(A) Structure-Activity Relationship (SAR) information of HUHS015 from its analog A15 and designed derivatives by extensive chemical modifications. (B–F) The chemical structures and potencies of A15 and its derivatives designed by SAR-guided modifications. The modifications include alterations in the ring structure fused with the hydroxypyrazole moiety (B), replacing the benzimidazole moiety with other types of heterocycles (C), substitutions and heteroatom incorporations in the phenyl group of the benzimidazole moiety (D), alterations in the ring structure fused with the hydroxypyrazole moiety of compound 36 (E), substitutions and heteroatom incorporations in the phenyl group of the benzimidazole moiety of compound 59 (F). The EC_{50} of all designed compounds are listed. (G) EC_{50} calculation plots for HUHS015, A15 and representative derivatives are shown.

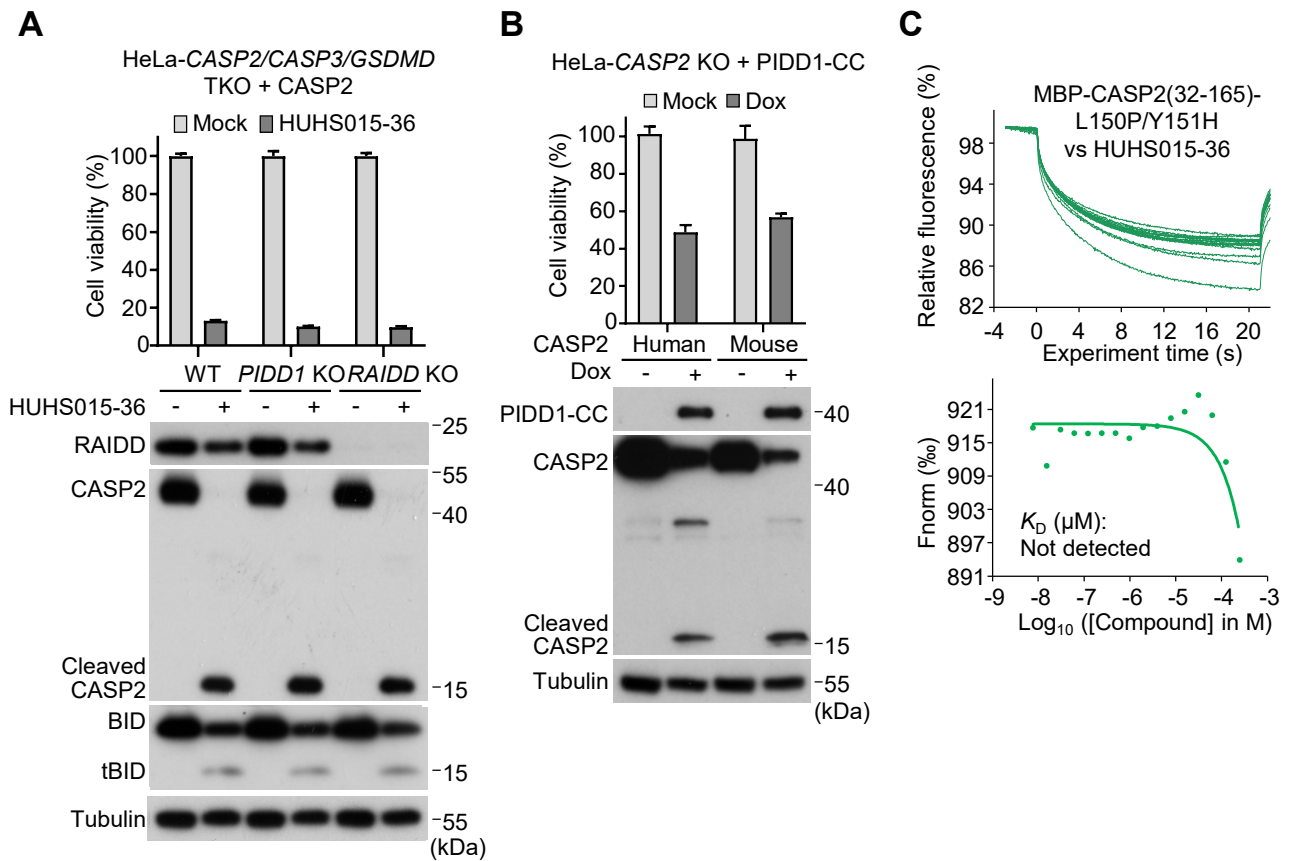


Figure S5. HUHS015-derived compound activates human caspase-2 in a different way from that for PIDDosome-mediated caspase-2 activation.

(A) HUHS015-36 activates caspase-2 independently of PIDDosome. WT, *PIDD1*^{-/-} (KO) and *RAIDD*^{-/-} (KO) HeLa cells with exogenous caspase-2 expression were treated with HUHS015-36 for 5 h. ATP-based cell viability is expressed as mean \pm s.d. from three technical replicates. Immunoblotting detecting caspase-2 and BID processing is shown. (B) PIDDosome activates both human and mouse caspase-2 to induce cell death. *CASP2*^{-/-} (KO) HeLa cells rescued with human or mouse caspase-2 expression were stimulated by dox-induced expression of PIDD1-CC. ATP-based cell viability is expressed as mean \pm s.d. from three technical replicates. Immunoblotting detecting PIDD1-CC expression and caspase-2 processing is shown. (C) Microscale thermophoresis (MST) detects no binding between HUHS015-36 and MBP-fused human caspase-2 pro-domain containing L150P/Y151H double mutations. MST profiles for raw binding signals and affinity (K_D) measurement are shown. All data are representative of three independent experiments.